Ann. Rev. Biochem. 1977. 46:299–329

STRUCTURE AND FUNCTION OF CYTOCHROMES C

◆948

F. R. Salemme

Department of Chemistry, University of Arizona, Tucson, Arizona 85721

CONTENTS

PERSPECTIVES AND SUMMARY

With few exceptions all organisms are primarily dependent upon transducing electron-transport chains for the production of adenosine triphosphate, the common high-energy chemical intermediate of living cells. Figure 1 shows schematically two representative examples of energy-transducing electron-transport chains: the oxidative chain of eukaryotic mitochondria and a cyclic photophosphorylating chain of photosynthetic bacteria. Such chains are typically composed of two functionally different types of electron carriers: those which are capable of conserving a change in the electromotive potential of a reducing electron as a chemically useful energized state (non-isopotential electron-transfer proteins) and others which serve to transfer electrons between the sites of energy conservation (isopotential

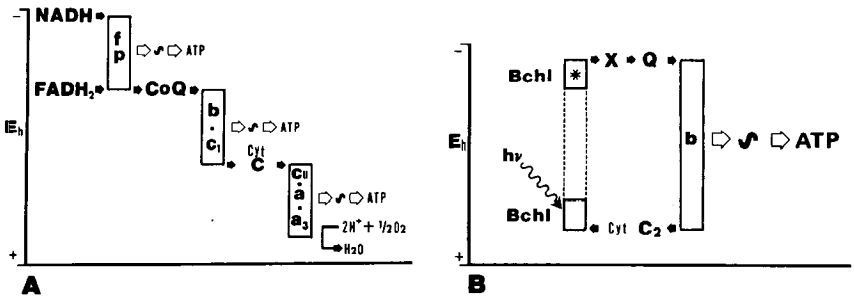

Figure 1 Energy-transducing electron-transport chains. Part *A* shows schematically the oxidative electron-transport chain of eukaryotic mitochondria, which utilize reduced cofactors as a source of low-potential reducing electrons, and oxygen as the final electron acceptor. Part *B* shows a cyclic bacterial photosynthetic electron-transport chain in which reducing electrons are created by the direct action of light. Solid arrows indicate isopotential electron transfers between isopotential electron carriers and membrane-bound energy-transducing proteins. Open arrows indicate sites of conservation of a change in reducing electron potential as "squiggle," an energized state required for ATP synthesis. In these and related energy-transducing chains, high-potential cytochromes *c* serve as isopotential electron donors to the most oxidizing protein electron acceptors.

electron carriers). The precise nature of the mechanisms by which specific electron transfer takes place to or from the isopotential carriers of these chains, or within the non-isopotential energy-transducing proteins, remains an unsolved biochemical problem of fundamental importance.

The protein electron carriers of these chains that have been most extensively investigated are the soluble high-potential cytochromes *c.* This class of small, ubiquitously distributed heme proteins includes eukaryotic mitochondrial cytochrome *c,* the bacterial photosynthetic cytochromes c_2, and several others of prokaryotic origin. Considerable amino acid sequence data exist which suggest that all of these proteins are descendants of a common evolutionary ancestor. Further evidence for the evolutionary relationship of these molecules derives from the analogous nature of their physiological function; i.e. high-potential cytochromes *c* generally function as isopotential electron carriers between a membrane-bound cytochrome *b* (or c_1) and the most oxidizing protein electron acceptor of their respective electron-transport chains (Figure 1). Several reviews have recently appeared that treat various aspects of the extensive literature on the chemical, physical, and biological properties of the cytochromes *c* (1–5). This review focuses on considerations of the mechanism of electron transfer and biological interaction of these proteins, based primarily on the available protein crystallographic structural information.

In general, the greatest advantage of the protein crystallographic technique, with respect to the elucidation of the catalytic mechanisms of enzymes, is that it provides a more or less direct means to examine the nature of the enzyme-substrate interaction. The cytochromes *c* cannot, however, be considered as enzymes in the conventional sense. Instead, they are best viewed as cofactors for the proteins with which they interact. Despite considerable evidence that the oxidized and reduced forms of the cytochromes differ physically, there are presently no indications from crystallographic structural studies that any covalent alterations or static conformational changes accompany oxidoreduction of these molecules. Further, direct structural examination of the complex interaction made between the cytochromes *c* and their physiological oxidoreductases has been precluded since these latter proteins are generally membrane-bound and hence not easily crystallized. This situation has made it difficult to identify structurally either the site of interaction or the mechanism of electron transfer in these proteins. Consequently, much of what is currently known about their function has derived from comparative studies of their structural, physical, and biochemical properties.

Taken together, the available data suggest that the cytochromes *c* form alternative associations with their membrane-bound physiological oxidoreductases, which are mediated by complementary-charge interactions formed between a common positively charged surface domain of the cytochromes *c* and corresponding negatively charged surface domains of their oxidoreductases. For the cytochromes *c* of known structure, the common positive charge domain is localized on a surface region of the molecules where the otherwise buried heme prosthetic group is most exposed to solvent, suggesting that both oxidation and reduction take place by a reversible mechanism involving direct interaction of the cytochrome *c* heme prosthetic group with those of its oxidoreductases (1). There is currently no consensus about whether electron transfer occurs spontaneously when the cytochrome *c* and oxidoreductase prosthetic groups attain the proper relative orientation and proximity, or whether electron transfer involves the sort of specific facilitation commonly encountered in enzymatic catalytic processes. At least one oxidoreduction mechanism has been proposed for a cytochrome *c*, *Rhodospirillum rubrum* cytochrome c_2, which is of the facilitated type (1). Although the evidence suggests that all cytochromes *c* undergo oxidoreduction by essentially reversible mechanisms involving direct heme involvement in the electron-transfer process, various members of this diversified class of molecules exhibit substantial differences in their physical and biological reactivity properties whose structural origin remains unclear. Consequently, further structural studies of these proteins are being actively pursued in several laboratories, in order to better define the specific

structural features that serve to regulate heme potential and give rise to the observed reactive specificity of these molecules. These comparative studies should provide useful information relevant to the mechanisms of the non-isopotential energy-conserving electron-transport proteins, as well as provide a unique opportunity to examine the structural and functional evolution of a class of molecules whose species diversification is essentially universal.

OCCURRENCE AND STRUCTURAL FEATURES OF HIGH-POTENTIAL CYTOCHROMES C

A *c*-type cytochrome is defined as a protein having one or more protoheme IX prosthetic groups covalently bound to the polypeptide chain by thioether linkages resulting from condensation of the heme vinyl groups with polypeptide cysteine sulfhydryl groups. Such cytochromes have historically been identified by their characteristic spectroscopic properties (5). There appears to be considerable diversity, especially evident among the prokaryotic organisms, in the structural and functional properties of these molecules as they have been defined (5). Indeed, the extensive amino acid sequence studies on the prokaryotic cytochromes *c,* which have been carried out principally by Ambler and co-workers, show that there are several subclasses of these proteins which bear little similarity beyond the presence of one or more covalently bound heme prosthetic groups (5–7). High-resolution crystallographic structural studies have thus far been confined to a subclass of molecules that are generally characterized as: (*a*) consisting of a single polypeptide chain of ~85 to ~135 residues, containing a single heme prosthetic group covalently bound near the amino terminus; (*b*) having histidine and methionine as the axial heme iron ligands; and (*c*) possessing relatively high oxidoreduction potentials in the range of +150 to +380 mV.

The members of this class of "high potential" cytochromes *c* include mitochondrial cytochrome *c,* the cytochromes c_2 of photosynthetic bacteria, and cytochromes c_{550} of denitrifying bacteria, as well as the generally smaller algal cytochromes *f, Pseudomonas* cytochromes c_{551}, *Chlorobium* cytochromes c_{555}, and several others of prokaryotic origin (2, 6, 7). The available amino acid sequence data suggest that the high-potential cytochromes *c* may have descended from a common evolutionary ancestor; nevertheless, there is evidence for considerable structural diversification among the prokaryotic members of this class (5–7). In contrast, the structure of mitochondrial cytochrome *c* appears to have been essentially fixed at the time of the emergence of the first eukaryotes and, indeed, is usually considered to be one of the most evolutionarily conservative proteins (2).

At present, three high-potential *c*-type cytochrome structures have been determined at high resolution: tuna heart mitochondrial cytochrome *c* (8, 9), *Rhodospirillum rubrum* cytochrome c_2 (10), and *Paracoccus denitrificans* cytochrome c_{550} (11, 12), whose structures are schematically shown in Figures 2–4. As can readily be seen from inspection of the drawings, these molecules have very similar overall tertiary configurations despite both the variable lengths of their polypeptide chains resulting from various insertions and deletions in their sequences, and the fact that they function in different types of electron-transport chains. Figure 5 shows a conjectural structure for a typical "small" prokaryotic cytochrome *c*, based on sequence analyses and low-resolution crystallographic studies on *Pseudomonas* cytochrome c_{551} (7) and *Chlorobium thiosulfatophilum* cytochrome

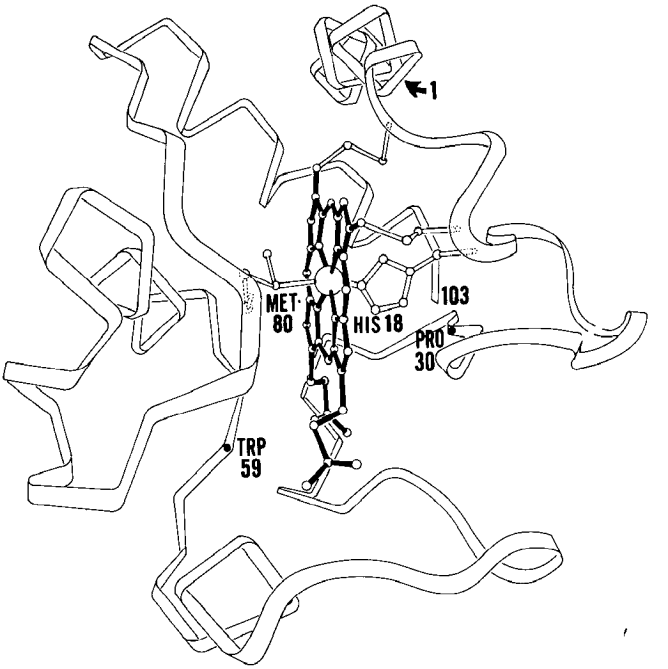

Figure 2 A schematic representation of a mitochondrial cytochrome *c* (tuna heart) as determined by R. E. Dickerson and co-workers (8, 9). There are five regions of α-helical secondary structure in the molecule including one near the amino terminus, a short stretch in the 50's region at the bottom of the molecule, two connected short helices in the 65–75 region at the left of the molecule, and a final helix at the carboxy chain terminus forming the upper rear of the molecule. Specifically designated residues appear most conservative among diverse species of high-potential cytochromes *c*.

c_{555} (F. R. Salemme, unpublished results). This structure differs principally from those shown in Figures 2–4 by the deletion of a loop forming the bottom of the larger cytochromes *c,* which is to some extent structurally compensated by an inward folding of a section of polypeptide located sequentially nearer the carboxy chain terminus in the smaller molecules. An overall sequential comparison summarizing the relationships between these cytochromes *c* is given in Figure 6. Collectively these molecules may be described as consisting of a single thickness of polypeptide chain having more or less α-helical secondary structure, which envelops the heme prosthetic group leaving only one edge relatively exposed to the solvent.

Figure 7 shows the heme environment in *R. rubrum* cytochrome c_2, which is overall very similar to that observed in both the mitochondrial and

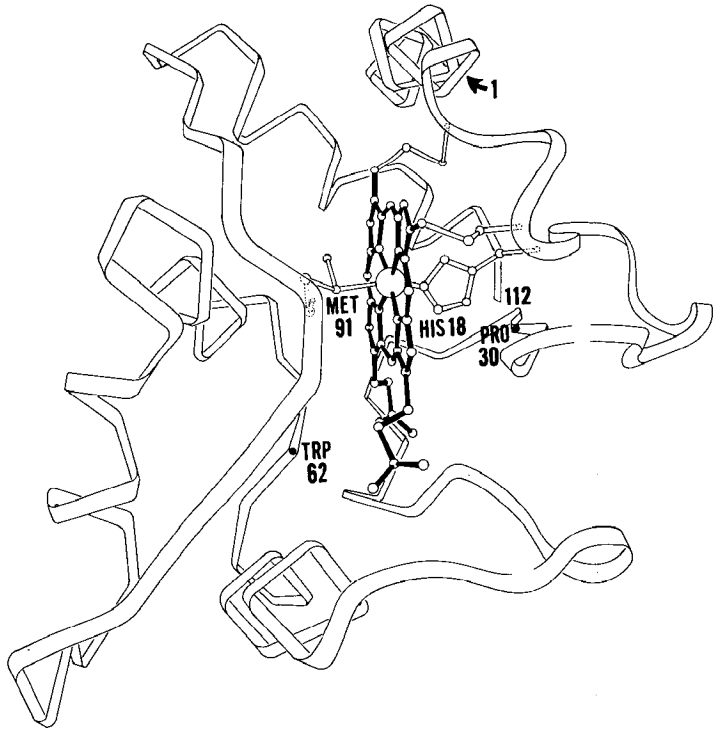

Figure 3 Schematic diagram of the photosynthetic cytochrome c_2 of *Rhodospirillum rubrum.* This structure differs from that of mitochondrial cytochrome *c* principally by a lengthening of the α-helices at the bottom and front left sides of the molecule. Recent sequence studies by Ambler and co-workers (6) indicate that there are other species of bacterial cytochrome c_2 that most probably closely resemble the mitochondrial cytochrome *c* structure shown in Figure 2.

the *P. denitrificans* cytochromes *c*. The heme iron forms axial coordinate bonds with two strong field ligands, a histidine imidazole nitrogen and a methionine sulfur, resulting in a low-spin heme iron complex that remains planar in both its oxidized and reduced states. There is an extensive pattern of both covalent and hydrogen-bonded interactions that serve to constrain the heme rigidly such that only one hydrophobic edge is exposed to solvent. Several of these hydrogen-bonded interactions are notable since the amino acids involved appear to be sequentially invariant among the larger cytochromes *c*. These include two hydrogen bonds formed between *R. rubrum* Trp 62 and Tyr 48 and the buried rear heme propionate, and a hydrogen bond formed between the fifth heme ligand histidine imidazole and the backbone carbonyl of Pro 30 (see Figure 6). The hydrogen bond formed

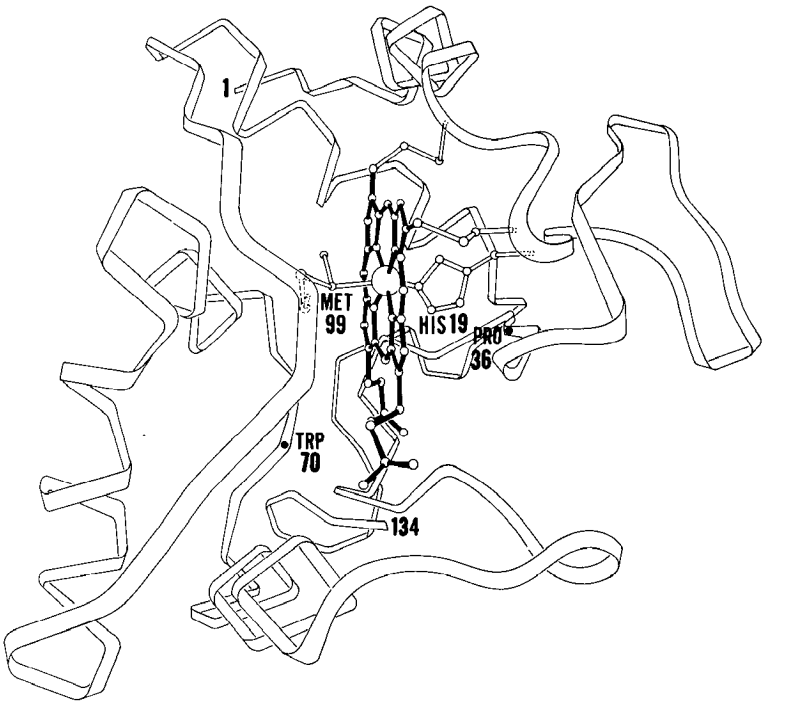

Figure 4 Schematic diagram of cytochrome c_{550} from the denitrifying bacteria *Paracoccus denitrificans* as determined by Timkovich & Dickerson (12). Relative to the structures shown in Figures 2 and 3, this molecule shows further elongation of the α-helices forming the bottom and left front of the cytochrome molecules, but additionally differs by the insertion of a loop of polypeptide at the right of the structure, and an elongation of the chain beyond the final α-helix at the rear of the molecule.

between the rear heme propionate and Trp 62 appears to be of particular importance in the maintenance of the integrity of the oxidized molecular structure, since chemical modification studies have indicated that structural alteration of this residue is accompanied by loss of the methionine heme ligand (1, 2, 13, 14).

In addition to the aforementioned covalent and hydrogen-bonded heme interactions, there are a large number of nonbonded hydrophobic heme interactions arising from the packing of internal aromatic and aliphatic amino acid side chains. Of the aromatic residues shown in Figure 7, those corresponding to *R. rubrum* Phe 20, Tyr 46, Tyr 48, Trp 62, Tyr 70, Phe 93,

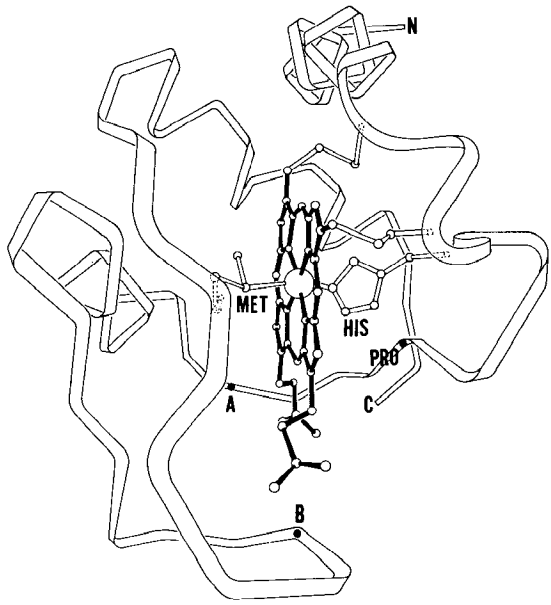

Figure 5 A conjectural structure for a small prokaryotic cytochrome *c* based on sequential and low-resolution structural studies on *Pseudomonas* cytochrome c_{551} (7) and *Chlorobium* cytochrome c_{555}. These structures generally appear to retain three of the helical regions common to the larger structures, but differ by a shortening of the right side loop, and an extensive chain deletion, which forms the bottom of the larger molecules. This latter deletion appears to be structurally accommodated by an inward folding loop of chain, which forms the left side of the cytochrome c_2 and c_{550} molecules. The sequential positions of a tryptophan that is conserved in the *Chlorobium* cytochrome c_{555}, *Pseudomonas* cytochromes c_{551}, and four of five algal cytochromes *f* are designated by the letters *A, B,* and *C,* respectively.

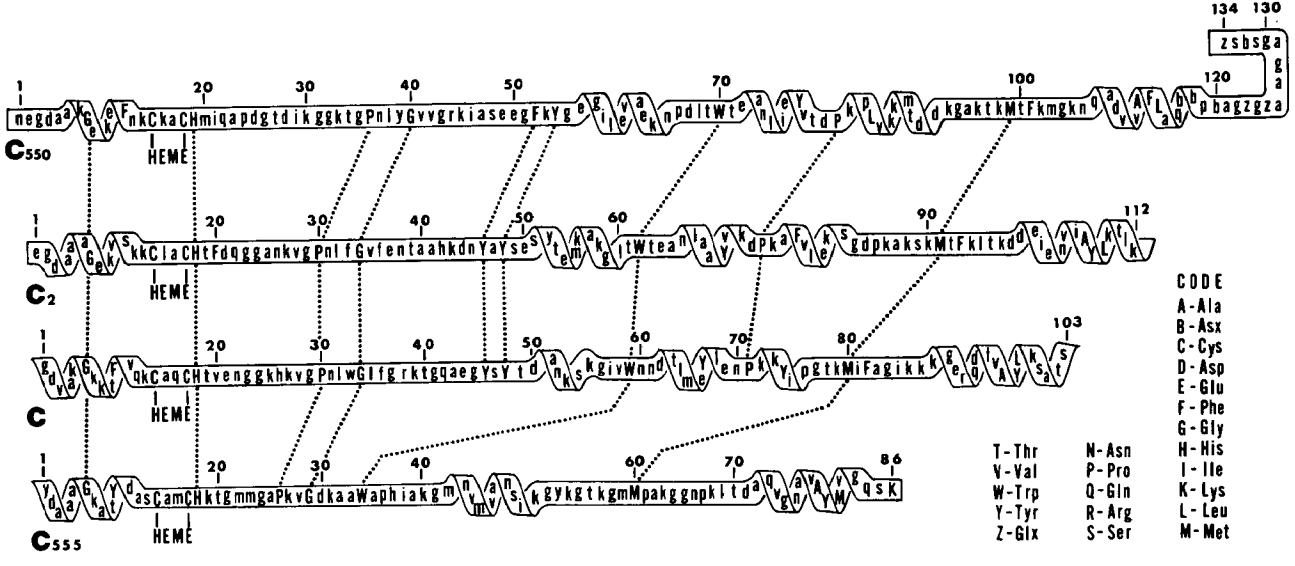

Figure 6 Sequence comparison of some representative cytochromes *c;* from the top *Paracoccus denitrificans* c_{550}, *Rhodospirillum rubrum* c_2, tuna heart mitochondrial *c,* and *Chlorobium thiosulfatophilum* c_{555}. Dotted lines connect structurally important or otherwise invariant residues (capitalized), as described in the text. Helical regions are shown to facilitate structural comparisons (Figures 2–5) and illustrate the evolutionary relationships between molecules. Helical designations for cytochrome c_{555} are largely conjectural.

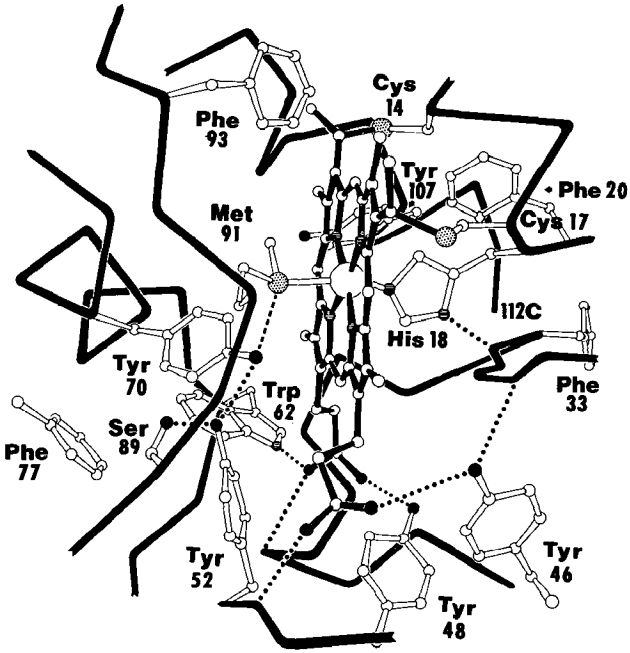

Figure 7 An illustration of the heme environment in *Rhodospirillum rubrum* cytochrome c_2, which is in most respects similar to that observed for mitochondrial cytochromes *c* and *Paracoccus denitrificans* c_{550}. The protoheme IX prosthetic group is attached to the polypeptide backbone chain (shown as a black wire) by four covalent bonds. Two bonds result from condensation of the heme vinyl groups with cysteine side chains to form thioether linkages. The remaining two are axial coordinate bonds formed between the heme iron and two strong field ligands, a histidine imidazole nitrogen (shaded) and a methionine sulfur atom (stippled). Current evidence indicates that the heme iron remains low-spin and in the plane of the heme in both its singly charged oxidized (Fe d^5) and its uncharged reduced states (Fe d^6). An extensive system of hydrogen bonds (dotted) serve to stabilize the buried heme propionic-acid side chains, although the overall environment of the heme crevice is hydrophobic due to the packing of aromatic (shown) and aliphatic amino acid side chains with the heme. The interaction of tryptophan-62, which donates a hydrogen bond to the rear heme propionate, is notable, since this heme interaction appears to be potentially conserved in almost all high-potential cytochromes *c* with the possible exception of some algal cytochromes *f* (see Figure 5).

and Tyr 107 appear to conserve their aromaticity in all of the larger cytochromes *c* of known sequence (Figure 6). In contrast, Tyr 52 is unique to *R. rubrum* cytochrome c_2; this sequence position is occupied by a variety of amino acids in related cytochromes *c* (2). Another unusual feature of *R. rubrum* cytochrome c_2 is that the invariant structural homologue of *R. rubrum* Phe 20 is located at sequential position 10 of the mitochondrial cytochromes *c*, as well as most other species of bacterial cytochrome c_2. Conversely, although residues 106–109 of the *R. rubrum* sequence show exact homology with those at positions 96–99 in tuna mitochondrial cytochrome *c*, *R. rubrum* Tyr 107 occupies a different spatial position from its sequential analogue in mitochondrial cytochromes *c*, Tyr 97. The difference in the spatial location of these sequentially homologous residues appears to be a result of a one-residue displacement of the cytochrome c_2 carboxy terminus helix relative to the carboxy terminus helices of either the mitochondrial or the *P. denitrificans* cytochromes *c* (1). The principal effect of this relative chain displacement is to locate Tyr 107 of *R. rubrum* c_2 quite close to the heme prosthetic group, whereas the homologues of this group are essentially solvent-exposed in the related cytochrome structures. These observations clearly point out the potential pitfalls of making structural extrapolations from a protein of known structure to another of unknown structure when their lengths and sequences are not virtually identical. Nevertheless, in light of the apparent importance of the interaction made between the homologues of *R. rubrum* Trp 62 and the cytochrome *c* heme, it is interesting to note that both the *Chlorobium* cytochromes c_{555} and the *Pseudomonas* cytochromes c_{551} contain sequentially invariant tryptophan residues at positions potentially allowing them to make heme interactions similar to those seen in the larger cytochromes (Figure 5).

The packing of aromatic and aliphatic amino acid side chains adjacent to the heme places it in a very hydrophobic environment. The hydrophobic nature of the heme environment, together with the nature of the iron ligands, probably accounts for the high oxidoreduction potentials of the cytochromes *c* relative to those observed for aqueous heme complexes. Presumably, the high potentials of the cytochromes reflect the difficulty of accommodating a positive charge on the buried ferricytochrome heme iron, which consequently tends to increase its affinity for a reducing electron (15, 16). It is possible that the difference in observed potential between mitochondrial cytochrome *c* ($E_{m,7} = +260$ mV) and *R. rubrum* cytochrome c_2 ($E_{m,7} = +320$ mV) may be accounted for by the differences in the hydrophobicity of their heme environments, since the heme crevice of *R. rubrum* cytochrome c_2 contains two tyrosine residues (52 and 107) that are not present in the heme crevice of mitochondrial cytochrome *c*. It is

equally likely, however, that such potential differences could arise from differences in the relative structural stabilities of the molecules in their oxidized and reduced states (17).

Although the observed potential differences between the mitochondrial cytochromes *c* and the photosynthetic cytochromes c_2 are not large (~60 mV), there are known cases where cytochromes *c* of the same size, showing no gross differences in overall amino acid composition, have quite different oxidoreduction potentials (e.g. *C. thiosulfatophilum* c_{555}, $E_{m,7} = +150$ mV, 86 residues; and *Euglena gracilis* cytochrome *f*, $E_{m,7} = +350$ mV, 86 residues) (5). The elucidation of the structural factors responsible for such potential differences between molecules that might otherwise be expected to be structurally similar is basic to an understanding of both the isopotential and the non-isopotential energy-conserving electron-transfer processes.

OXIDATION-REDUCTION MECHANISMS

General Considerations

Electron-transfer reactions between coordinate metal complexes can generally be considered to proceed by one of three mechanisms.

1. Reactions of two complex metal ions in which one or more of the ligands become common to the coordination shells of both reacting species are termed inner-sphere electron-transfer reactions. Although cytochromes *c* are known to undergo reduction by inner-sphere mechanisms with inorganic reducing agents (3, 4), there is currently no evidence for any ligand exchange accompanying heme oxidoreduction under physiological conditions (18). This, together with the structural observation that the heme iron is inaccessible from the exterior of the molecule, suggests that inner-sphere mechanisms are unlikely to be involved in the physiological oxidoreduction of these molecules.

2. Reactions of two complex ions that throughout their entire course maintain the integrity of the coordination shells of the reacting species are termed outer-sphere electron-transfer reactions. Implicit in the definition of outer-sphere processes is the idea that electron transfer can take place via molecular orbitals delocalized throughout the reactant metal complexes. Crystallographic structural studies show that the cytochrome *c* heme is accessible to the surface at one edge, which could potentially allow orbital overlap between the conjugated heme π orbital system and that of the prosthetic group of a physiological oxidoreductase. In addition, nuclear magnetic resonance studies indicate considerable electron spin-density delocalization over the ferricytochrome *c* heme (18). Together these observa-

tions suggest that the cytochromes *c* possess the requisite physical and structural features to undergo oxidoreduction by an outer-sphere reaction mechanism (1, 3, 4, 17, 19). It is consequently appropriate to examine the structural implications of this well-developed theory (20) as a prelude to a discussion of the specific proposals made for the mechanism of cytochrome oxidoreduction. Figure 8 shows a potential surface-reaction coordinate diagram for an outer-sphere isopotential electron-transfer reaction between two complex metal ions that differ only in the oxidation states of their metals [e.g. $Fe(CN)_6^{-4}$ is *D*, $Fe(CN)_6^{-3}$ is *A*]. The shapes of the potential surfaces for the isolated reactant donor (*D*) and acceptor (*A*) molecules

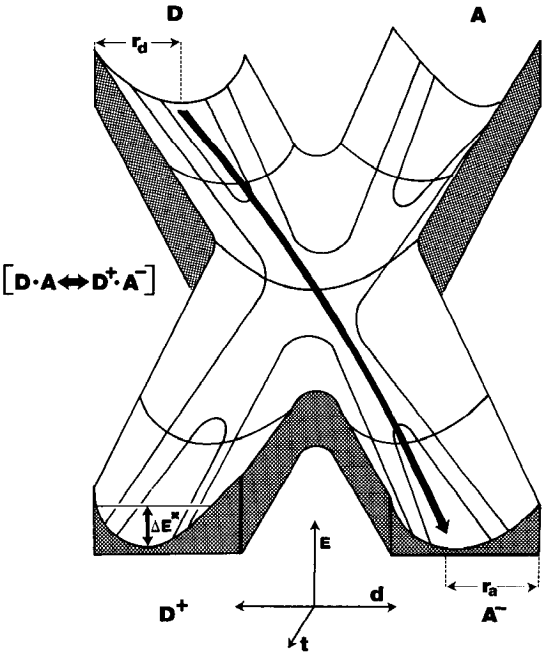

Figure 8 A potential surface-reaction-coordinate diagram for an isopotential outer-sphere electron-transfer process between two complex metal ions differing only in metal oxidation state [e.g. $Fe(CN)_6^{-4}$ is *D*, $Fe(CN)_6^{-3}$ is *A*]. The shapes of the surfaces represent spatially averaged potential fields as a function of distance from the complex centers. As shown, the reducing electron resides at r_d in the isolated donor complex. Approach of the donor and acceptor species involves work terms arising from electrostatic interactions, solvent stripping and rearrangement, and rearrangement of the reactant configurations to form the symmetrical transition state. The sum of these work terms is the activation energy for the reaction, ΔE^*. Electron transfer takes place in a non-energy-requiring process, and the system proceeds to products, which in this case are isostructural with the reactants (i.e. $r_d = r_a$).

represent three-dimensionally averaged potential fields as a function of distance from the respective complex centers. As shown, the isolated donor electron occupies a minimum energy configuration at radius r_d. Approach of the donor and acceptor species to attain the transition state involves several types of work terms whose sum equals ΔE^*, the activation energy. These work terms arise from (*a*) electrostatic interactions between the approaching reactants, (*b*) solvent stripping and ion rearrangements, and (*c*) rearrangement of the configuration of the reactants to form the symmetrical transition state. Electron transfer then takes place in an non-energy-requiring process and the system subsequently goes to products by the converse route required to attain the transition state ($r_d = r_a$).

3. Another mechanism that has been periodically invoked to explain biological electron-transfer processes is quantum mechanical tunnelling. This mechanism derives from the quantum mechanical consideration of the electron as a wave packet that has a finite probability of penetrating any potential barrier it might encounter; for example, according to the equation

$$K = \nu \exp\{-4\pi/h[2m\Delta E]\alpha^{1/2}\},$$

where K is the rate of electron flow through the barrier, ν is the frequency of encounter of the electron wave packet with the barrier, h is Planck's constant, m is the electron mass, ΔE is the barrier height, and α is the barrier width. Most applications of this formula to biological problems have been directed toward calculating α, the barrier width or supposed separation between the electron donor and acceptor sites. A basic problem accompanying the direct application of this formula, aside from assigning accurate values to the various parameters (21), is that it has no temperature dependence, in contrast to the situation actually found for most biological electron-transfer reactions. A more recent treatment by Hopfield (21) overcomes this difficulty by assuming coupling of thermally activated molecular vibronic states to electronic states during tunnelling between statically oriented electron donors and acceptors. Application of this theory to data on the photooxidation of *Chromatium* cytochrome c_{552} gave a distance of 8–10 Å for the separation of electron donor and acceptor sites in this system, a value that is significantly less than those calculated by other methods (20–50 Å) and more in keeping with the observed specificity of biological electron-transfer reactions, which presumably must arise from direct interaction between the reacting species.

A simplified picture of how a "thermally activated" tunnelling process might occur for an isopotential electron-transfer process between two reversibly associating molecules is shown in Figure 9. The surface shown is not a classical surface, but rather a definition of the potential well that confines the electron during the course of the reaction. In an isolated donor

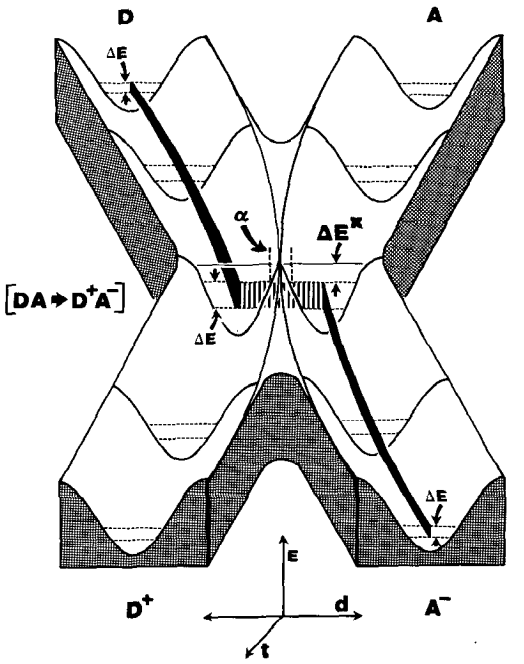

Figure 9 A reaction-coordinate diagram for a thermally activated short-range tunnelling process. The surfaces shown here represent the shape of the potential wells confining the electron wave during the course of the reaction. In the isolated electron donor *D,* the electron resides in an energy band whose bandwidth ΔE is coupled to the thermally activated vibrational modes of the molecule. As the donor collides with the acceptor *A,* the translational kinetic energy of the reactants is transiently conserved, leading to an increase in the energy of the internal vibrational modes of the transition state complex. This results in an increase in electron energy bandwidth, and an effective reduction in the height of the tunnelling potential barrier, ΔE^*. Short-range tunnelling (shown by the vertically striped path) then takes place through the barrier of width α, and the system proceeds to products. Here the electrostatic interactions and solvent rearrangement processes are shown to result in a change of the shape of the potential wells during the course of the reaction. Such changes in potential well shape also affect both the electron energy bandwidth and the average energy of the electron in the well.

molecule the electron resides in an energy band whose width, ΔE, is coupled to the frequency of the internal thermally induced vibrations of the molecule. When the donor molecule collides with the acceptor, conservation of the translational kinetic energy of the reacting species results in an effective increase in energy of the internal vibrational modes in the molecular complex. The increase in the energy of the internal vibrational modes

of the complex is coupled to the electronic state of the donor molecule and serves to effectively reduce ΔE^*, which here represents the quantum mechanical barrier height. This results in a short-range tunnelling event, after which the thermally activated transition state is rapidly dissipated by the solvent, leading to product formation. The electrostatic and solvent rearrangement processes accompanying the reaction are shown here to manifest themselves by a change in the shape of the potential well confining the electron, i.e. as the solvent is stripped off the closely approaching molecules, the potential wells become altered because of the changing local environment.

There are two features of both the outer-sphere and the short-range tunnelling mechanisms that are relevant to the reactions of biological electron carriers. First, since both mechanisms require close approach of the reacting molecules, they will be affected by the nature of the charge and tenacity of the hydration spheres of the reacting species. Although these factors present energetic barriers for the formation of the transition state for well-solvated molecules of like charge, reactions of poorly solvated molecules of unlike charge will be facilitated. Second, in both mechanisms some degree of structural or electronic distortion of the reactants accompanies formation of the transition state. Clearly, if the interactions made between the polypeptide chain and the prosthetic group of a biological electron-transport protein can induce the required distortions either in the isolated molecules or when they initially form a complex, this will also serve to facilitate the electron-transfer reaction.

An additional factor of importance in biological electron-transfer mechanisms, which is not explicitly emphasized in the preceding descriptions since they describe only productive molecular collisions, is the necessity that the prosthetic groups of reacting biological molecules attain the proper relative orientations prior to electron transfer. Indeed, attainment of the proper relative orientation between reacting species as dictated by precise structural interactions generally provides an important basis for both the specificity and the catalytic efficiency of biological processes.

Proposals for Oxidoreduction Mechanisms in Cytochromes c

The first structural proposal for a specific cytochrome oxidoreduction mechanism was made by Dickerson and co-workers on the basis of the structure determination of horse and tuna heart mitochondrial cytochrome *c* in their oxidized and reduced states, respectively (22–25). In this mechanism, reduction of the heme was proposed to take place by a series of free-radical transfers involving an external tyrosine residue 74 located at the left surface of the molecule, which subsequently transferred an electron to

an internal Tyr 67 and/or Trp 59 side chain adjacent the heme, which in turn led to heme reduction. Oxidation of the protein was proposed in the earlier versions of this mechanism to take place by a similar free-radical mechanism involving two aromatic residues (Phe 10 and Tyr 97) located to the right of the heme. A subsequent version involved direct heme oxidation via its relatively exposed edge at the front surface of the molecule. This mechanism was principally based on the sequence invariance of the aromatic residues involved among all known species of mitochondrial cytochrome *c* (some 50), as well as apparent differences in the relative orientations of these aromatic residues in the oxidized and reduced molecular structures.

An attractive feature of this mechanism involving independent reduction and oxidation pathways was the suggestion that a statically oriented cytochrome *c* molecule could serve as a direct electron conductor between its physiological reductase and oxidase. Objections to this proposal were made on energetic grounds (1) because physical-chemical studies (26, 27) suggested that the formation of a free-radical anion from a protein aromatic side chain required a reducing potential of about –3 eV (69 kcal). This seemed an unusually high energy of formation for what must, due to Frank-Condon restrictions, be a series of chemical intermediates in a reaction whose overall free energy change is close to zero. Additionally, it appeared that this reduction mechanism could not be reconciled with the observed structural and reactivity properties of the photosynthetic cytochrome c_2 of *R. rubrum.* Specifically, while cytochrome c_2 possessed aromatic residues that were sequentially homologous to those involved in the free-radical reduction scheme presented above, the residue corresponding to Tyr 74 in mitochondrial cytochrome *c,* Phe 77 in cytochrome c_2, was inaccessible from the molecular exterior (1). Nevertheless, cytochrome c_2 was reduced by mitochondrial cytochrome *c* reductase at 70% of the rate observed for cytochrome *c* (28, 29). In addition, crystallographic studies of cytochrome c_2 in both the oxidized and the reduced states revealed no significant conformational differences accompanying the oxidoreduction process, despite the fact that cytochrome c_2 exhibits phenomenological characteristics similar to those associated with oxidoreduction-coupled conformational change in cytochrome *c* (see below).

Subsequent crystallographic studies on both mitochondrial cytochrome *c* (8, 9) and *P. denitrificans* cytochrome c_{550} (12) have shown that these molecules also do not undergo any significant conformational change on oxidoreduction. Indeed, the recent observation that *P. denitrificans* cytochrome c_{550} lacks the initial member of the proposed aromatic free-radical chain (Tyr 74 in mitochondrial cytochrome *c* is structurally homologous to Leu 85 in c_{550}, Figure 6), while possessing good reactivity with the mito-

chondrial cytochrome *c* reductase (2), leads to the conclusion that the free-radical-chain mechanism is not operative in the physiological reduction of the cytochrome *c* (2, 12).

An alternative to the mechanism described above, which was first suggested for *R. rubrum* cytochrome c_2, proposed that heme oxidoreduction took place by an essentially reversible process involving direct interaction between the cytochrome c_2 heme and the prosthetic groups of both its physiological oxidase and its reductase (10). It was further suggested that electron transfer to or from this protein was not a passive process, but instead was specifically facilitated by a system of interactions that destabilized the existing heme oxidation state concomitantly with the association of cytochrome c_2 with its physiological oxidoreductases. The existence of such a system of interactions serving to facilitate heme oxidoreduction was inferred from examination of the 2.0-Å resolution structure of the oxidized molecule, where it appeared that the sixth heme iron ligand, the sulfur of Met 91, was slightly displaced off-axis toward the hydroxyl oxygen of the buried Tyr 70, which was in turn hydrogen-bonded through Tyr 52 to Ser 89 located at the front surface of the molecule (Figure 7). The off-axis displacement of the Met 91 sulfur was interpreted as being due to the existence of a partial ionic interaction between the hydroxyl oxygen of Tyr 70, bearing a partial negative charge, and the sulfur of Met 91, bearing a partial positive charge delocalized from the oxidized heme iron.

This system of interactions was proposed to offer stabilization to the oxidized heme state, and it suggested that interactions occurring upon association of the cytochrome c_2 molecule with its oxidoreductases could perturb the extent of this stabilization by influencing the state of protonation of Ser 89, thus facilitating heme oxidoreduction (Figure 10). This proposal appeared consistent with the observed pH versus midpoint-potential behavior of *R. rubrum* cytochrome c_2 (30), which shows a steady decline in potential between pH 5 and 8, suggesting successively decreasing protonation of Tyr 70 via Ser 89 as the pH is raised; this results in increasing stabilization of the oxidized state relative to the reduced state and a shift to a lower observed potential.

Although mitochondrial cytochrome *c* does not show a pH dependence of its oxidoreduction potential in the physiological pH range (31), early reports of the mitochondrial cytochrome *c* structure (22–25) indicated the presence of a hydrogen bond system similar to that observed in *R. rubrum* cytochrome c_2, with the exception that the homologue of *R. rubrum* Ser 89, Thr 78, was directly hydrogen-bonded to the hydroxyl of the tyrosine (Tyr 70 in c_2, Tyr 67 in cytochrome *c*) adjacent to the heme ligand methionine. It was subsequently proposed that oxidoreduction of mitochondrial cytochrome *c* could take place by a facilitated mechanism involving tran-

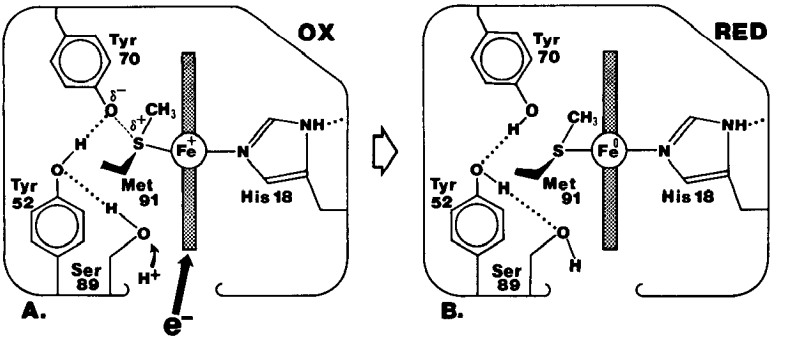

Figure 10 A facilitated mechanism for the oxidoreduction of *Rhodospirillum rubrum* cytochrome c_2. Part *A* shows schematically the oxidized state of the molecule in which some of the buried heme iron charge is delocalized to the sulfur atom of the sixth-ligand methionine sulfur. The oxidized iron state is stabilized by the formation of a partial ionic interaction of the methionine sulfur with a tyrosine hydroxyl bearing a partial negative charge, resulting from its participation in a hydrogen bond network that can delocalize the charge to the molecular surface at serine-89. Association with the physiological reductase involves perturbation of the hydrogen-bonding system stabilizing the oxidized iron, thus facilitating heme reduction (*B*). Perturbation of the stabilizing hydrogen-bond system could result from specific interactions affecting the state of protonation of serine-89, or alternatively could arise from neutralization of the high positive-charge density at the front surface of the molecule, which could also modify the affinity of serine-89 for a proton. Oxidation takes place by the reverse of the reduction process in this mechanism, which requires that the cytochrome be reversibly and alternately bound to its physiological oxidase and reductase. The true geometry of the interactions involved in this mechanism is shown in Figure 7.

sient perturbation of this hydrogen bond system, in principal similar to that proposed for *R. rubrum* cytochrome c_2 (1). However, the generality, if not the substance, of this facilitated mechanism is questionable in light of some recent observations. Of the 77 high-potential cytochromes *c* of known sequence that can be closely related to those of known structure, three do not possess hydrogen-bonding homologues to either *R. rubrum* Tyr 70 or Ser 89. Instead; *Euglena* cytochrome c_{558} has phenylalanine substituted for the tyrosine situated adjacent to the heme. Curiously, this cytochrome also lacks the covalent thioether heme linkage at position 14 (Figure 7) and shows anomalous biological reactivity properties (1, 2, 29). The cytochromes c_2 of *Rhodopseudomonas spheroides* and *Rhodospirillum molischianum* lack hydrogen-bonding homologues to *R. rubrum* Ser 89, although *R. spheroides* c_2 shows a similar pH dependence to that observed for *R. rubrum* cytochrome c_2 (17). Further, the more recent crystallo-

graphic studies on the mitochondrial and *P. denitrificans* cytochromes *c* do not clearly indicate the presence of a hydrogen bond from the heme-adjacent tyrosine hydroxyl group to a surface threonine residue side chain (8, 9, 12).

In summary, it is not currently possible to assign a general facilitated mechanism either to the high-potential cytochromes *c* of known structure or to those whose structure is inferred from sequence homology, which involves the specific participation of invariant amino acid residues. This is perhaps to be expected, given the differences in physical properties (17, 30, 32–37) and biological reactivities (2, 29, 38, 39) of these evolutionarily diversified molecules. Consequently, the high-resolution determinations of the structure of the smaller prokaryotic cytochromes *c* are eagerly awaited, since they are likely to have internal arrangements quite different from those of known structure, and hence might provide additional clues to the origin of the reactivity and specificity of these molecules.

INTERACTIONS WITH PHYSIOLOGICAL OXIDOREDUCTASES

Comparative Structural Studies

A fundamental feature of the mechanism described immediately above, which differentiates it from the free-radical-chain mechanism described earlier, is that both oxidation and reduction of the cytochrome is viewed to take place at the front side of the molecule where the heme is most exposed to solvent. Oxidoreduction of the cytochrome consequently requires that it be alternatively and reversibly bound to its physiological reductase and oxidase. There is currently a wide variety of data indicating that the interaction of the cytochromes *c* with their physiological oxidoreductases is primarily mediated by complementary charge interactions (29, 40–46). An observation of particular significance is that the reaction of mitochondrial cytochrome *c* with both its cytochrome oxidase and its reductase is completely inhibited in the presence of stoichiometric amounts of polylysine (29, 47). However, this fact is of relatively little use in the establishment of the site of interaction between the mitochondrial cytochromes *c* and their oxidoreductases because the molecule has a preponderance of surface positive charges as reflected by its strongly basic isoelectric point of 10.0. In contrast, *R. rubrum* cytochrome c_2 exhibits an isoelectric point of 6.2 (48) reflecting an approximately equal number of positive and negative charges on its molecular surface. Structural examination of the cytochrome c_2 molecule showed that the surface charge was very asymmetrically distributed, with 11 of the 17 total lysine residues forming an uninterrupted ring of positive charges about the perimeter of the heme crevice. Further, it

appeared that these residues were largely structurally or sequentially conserved in the mitochondrial cytochrome *c* structure, where they also formed the largest contiguous patch of surface positive charge (Figure 11). The subsequent determination of the *P. denitrificans* cytochrome c_{550} structure (12) shows that this protein possesses a similar extended region of positive charge localized at the front surface of the molecule, although it is not currently clear from amino acid sequence evidence that this extensive region of surface positive charge is conserved in some of the smaller prokaryotic cytochromes *c* (7).

Tests of the effects of polylysine on the reactivity of *R. rubrum* cytochrome c_2 with mitochondrial cytochrome oxidase, with which it reacts at about 5% of the rate of mitochondrial cytochrome *c*, and with the mitochondrial cytochrome *c* reductase, with which it reacts at 70% of the rate observed for mitochondrial *c*, showed, however, that both oxidation and reduction of cytochrome c_2 were effectively inhibited (29). These results were taken as substantive evidence that the site of interaction between the cytochromes *c* and their physiological oxidoreductases was at the front of these molecules, which in general show the greatest overall similarity in both their structures (Figures 2–6) and their surface charge distribution (Figure 11) and provide the only means for direct access to the heme prosthetic group.

A Hypothetical Model for a Protein Electron-Transfer Complex

As mentioned previously, it is currently not possible to examine crystallographically a complex of a cytochrome *c* bound to a physiological oxidoreductase. Recently, however, a modeling experiment (49) was carried out to test the structural reasonability of the proposal that the electron transfers mediated by cytochromes *c* take place by mechanisms involving essentially direct interactions between the cytochrome *c* heme prosthetic group and the prosthetic groups of the corresponding oxidoreductases. The objective of this experiment was to find the best complementary mechanical fit between tuna mitochondrial cytochrome *c* and microsomal cytochrome b_5 (50, 51). The selection of these molecules for this study was based on a variety of structural and biochemical observations. First, the oxidoreduction reactions of both cytochromes *c* and cytochromes b_5 (52) are observed to be strongly dependent on ionic strength, consistent with the structural observations that the heme crevice perimeters of the cytochromes *c* of known structure are populated by large numbers of sequentially and/or structurally conserved lysine residues, whereas the heme crevice perimeter of the cytochrome b_5 is populated by invariant negatively charged groups (51). Second, cytochrome b_5 is known to reduce cytochrome *c* at rates

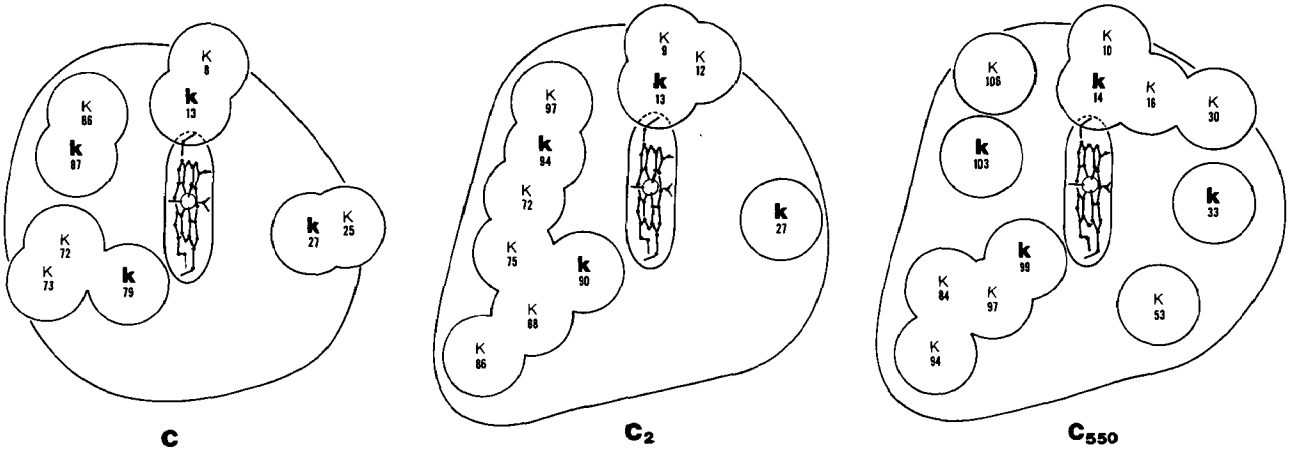

Figure 11 Front-surface positive-charge distributions on mitochondrial cytochromes *c*, *Rhodospirillum rubrum* c_2, and *Paracoccus denitrificans* c_{550}. The cytochromes *c* of known structure show in common an extensive distribution of surface positive-charged residues (lysine, K) about the perimeter of their heme crevices. As the isoelectric points of the c_2 and c_{550} cytochromes are nearly neutral, this constitutes a very asymmetric surface charge distribution on these molecules, in contrast to the situation for mitochondrial cytochrome *c*, which has a large preponderance of basic surface residues (pI = 10.0). Bold letters indicate those surface lysine residues which appear most structurally or sequentially invariant among the larger cytochromes *c*.

comparable to those observed for the physiological oxidoreductions of both molecules in their native environments (53). Although the question of whether cytochrome *c* functions as a physiological oxidant of cytochrome b_5 remains controversial, these observations suggest that an investigation of the potential structural complementarity of the cytochrome *c* and b_5 molecules would at the least define the minimum approach distance between the prosthetic groups of protein molecules known to react readily with each other. The possibility that the cytochrome *c*–cytochrome b_5 interaction might be physiologically significant, or at least structurally typical of such interactions, provided an additional basis for the experiment.

Figure 12 shows drawings representative of the surface topographies of the cytochromes *c* and b_5 molecules, which were generated by connection of the most exposed atoms (54) of surface amino acid residues to form irregular polyhedra. In order to find the best mechanical fit between the molecules, a least-squares fitting procedure was carried out that optimized potential complementary-charge interactions between the front-side positively charged invariant groups of cytochrome *c* and the front-side negatively charged invariant groups of cytochrome b_5, together with potential nonbonded intermolecular interactions in the interface region. There are four principal complementary-charge interactions formed in the best-obtained complex (Figure 13), which together with nonbonded interactions at the intermolecular interface serve to constrain the two hemes in nearly parallel orientations; the closest interatomic approach distance between heterocyclic π-bonded atoms of the two hemes is approximately 8 Å.

There are several features of this hypothetical complex that bear examination in light of the previous general discussion of classical outer-sphere and quantum-mechanical-tunnelling electron-transfer processes. Insofar as a strong ionic strength dependence of the oxidoreduction rate has been found to be a general property of reactions of reversibly bound electron carriers with their physiological oxidoreductases, it is first appropriate to consider the origin of the forces leading to the initial formation of the complex. The relevant structural observation is that the interacting charge groups in the cytochrome *c*–b_5 complex are members of larger surface-charge domains on the respective molecular surfaces (Figure 12), which are of *like* charge. Since the tertiary conformation of these molecules constrains these groups of like charge in close proximity to each other, this creates a situation in which ionic bond formation can compete with the usual water hydration of such groups, leading to formation of the complex. Thus formation of the complex can essentially be compared to crystallization of an ionic solute, which takes place when the solute concentration becomes so high

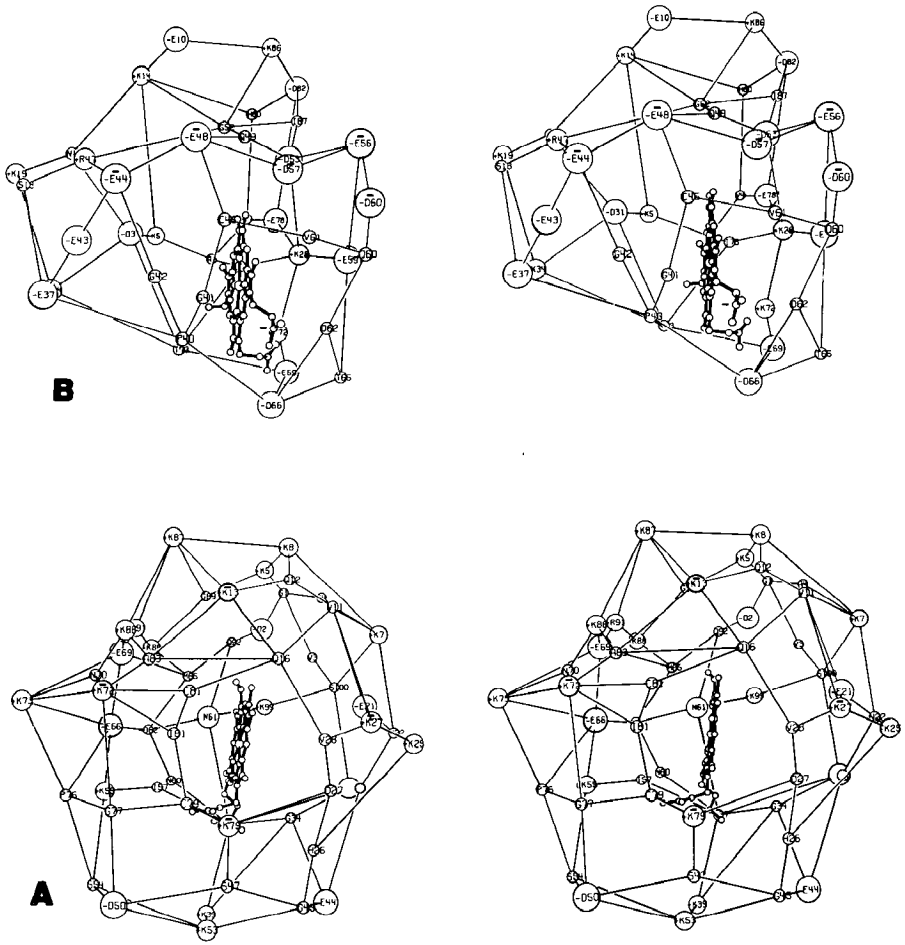

Figure 12 Polyhedral surface maps of the cytochrome *c* (*A*) and cytochrome b_5 (*B*) molecules. Surface residues were defined by the position of the most exposed atom, except in the case of acidic side chains, which were defined by the carboxylic carbon atom position, and are indicated by charge, residue, and sequence number. Some additional atoms not conforming to this labeling pattern define better the local surface topography of the respective heme crevice perimeters. These are for cytochrome *c:* O27 (Lys 27 peptide oxygen), C79 (Lys 79 C_γ), C81 (Ile 81 $C_\gamma 1$); for cytochrome b_5: C45 (Ile 45 $C_\gamma 2$), O60 (Asp 60 peptide oxygen), O62 (Gly 62 peptide oxygen). A heavy bar denotes essential charge invariance in all species of cytochrome b_5 and about 50 species of eukaryotic cytochrome *c*. Single-letter amino acid code is given in Figure 6.

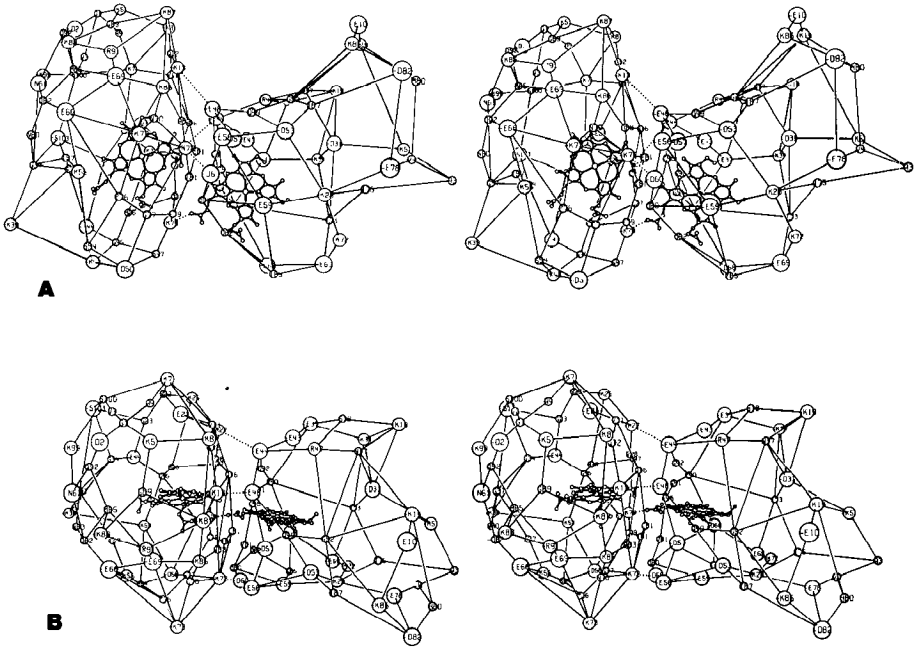

Figure 13 Polyhedral surface maps of the intermolecular complex of cytochromes *c* and b_5, showing side (*A*) and top (*B*) views. Cytochrome *c* is on the left of the complex. Dotted lines show principal charge interactions from charge group positions defined by original coordinate sets. The best fit shown was obtained allowing free rotation of lysine side chains of cytochrome *c* about the C_β-C_γ side-chain bond.

that there is no longer sufficient water to allow optimal hydration of solute ions. As a result, the solute is forced to make an alternative set of stabilizing ionic interactions and it crystallizes.

The complementary ionic interactions formed in the molecular complex not only provide the driving force for its formation, but also, together with the nonbonded interactions at the intermolecular interface, serve to constrain the hemes in nearly parallel orientations, a situation that is most propitious to the transfer of an electron from the delocalized π orbital system of the cytochrome b_5 heme to that of the cytochrome *c*. Additional consequences of complex formation are the neutralization of the charge groups at the intermolecular interface and the exclusion of bulk solvent water from this region. Together these lead to a significant reduction in the dielectric constant along the most direct path of interheme communication, consequently deshielding the hemes relative to their situation in the isolated

molecules and facilitating their interaction. In the context of the outer-sphere and short-range tunnelling mechanisms described earlier, it appears that the intermolecular complementary ionic interactions at once provide the driving force for complex formation, contribute to the proper relative orientations of the reacting prosthetic groups, and result in a change of dielectric constant in their environment, all of which serve to facilitate the electron-transfer process.

A final property of this hypothetical complex, which is of mechanistic interest, is the observation that the closest observed interatomic approach distance between resonant heterocyclic atoms of the heme is approximately 8 Å, a distance that is several angstroms longer than expected for a classical outer-sphere reaction involving orbital overlap between the reacting species, but close to the estimated range of a thermally activated tunnelling process (21). However, it is not realistic to attempt to distinguish between these mechanisms, which may ultimately turn out to be alternative mathematical descriptions of the same physical process, on the basis of the closest approach distance obtained in this model study. Rather it is possible, and even likely, that the formation of the transition-state complex in biological electron-transport proteins is accompanied by some degree of transient structural distortion such as is proposed to take place in classical outer-sphere reactions between inorganic metal ion complexes. Assuming that an outer-sphere electron transfer can take place at a closest interatomic approach distance of 3 Å between resonant π-bonded heme atoms, formation of the transition state in this hypothetical complex would necessitate relative distortions of about 2.5 Å between each polypeptide chain and its heme. The attainment of a transient distortion of this extent is not unreasonable and could probably be accommodated by appropriate movements of surface amino acid side chains in the complex interface region. Nevertheless, the possibility that biological electron transfer can take place over ranges somewhat longer than those required for outer-sphere mechanisms cannot be ruled out, since *Chromatium* high-potential iron protein, whose iron-sulfur prosthetic group is completely inaccessible to solvent (55), is known to react readily with cytochromes *c* (56).

OXIDATION STATE–COUPLED STRUCTURAL CHANGES

An extensive body of physical and chemical data exists which indicates that the structure of cytochrome *c* in some way differs in its oxidized and reduced states. This includes studies on the susceptibility of the protein to proteolytic digestion (57), various denaturing conditions (58–63), or heme

ligand substituents (64–66), as well as deuterium-exchange (67, 68), ion-binding (69–75), and calorimetric studies (76). Collectively, these observations suggest that the reduced form of cytochrome *c* possesses a more compact and structurally stable tertiary configuration than the oxidized form. However, there is currently no evidence from crystallographic data on the three cytochromes *c* of known structure that any significant conformational change accompanies a change in the heme oxidation state in these molecules. This situation deserves comment in light of the frequency with which the term "conformational change" has been used to describe the difference between the oxidized and reduced states of these molecules. All of the experimental approaches mentioned have the common characteristic that they measure what is, compared to the duration of a molecular vibration, a time-averaged property of the molecule. Consequently, from the solution studies it is not generally possible to distinguish whether the observed difference in properties of the oxidized and reduced molecules is due to a concerted change in the relative configurations of parts of the molecule (a static conformational change), or to a change in either the frequency or the amplitude of the vibrational modes of the structure (a dynamic conformational change). The crystallographic results indicate that the oxidoreduction-coupled conformational change of the cytochromes *c* is of the dynamic type, since a concerted static conformational change should be structurally observable.

One probable origin of the force resulting in the increased structural rigidity of the reduced form of the cytochromes *c* is the 100- to 1000-fold increase of coordinate bond strength of the sixth-ligand methionine sulfur-heme iron bond, which accompanies heme reduction (77). As can be seen from Figures 2–6, this bond provides one of the three covalent linkages holding the left and right sides of these molecules together. The importance of this bond in maintaining the structural integrity of the molecule is indicated by both chemical modification studies (3, 78, 79) and recombination studies (80, 81) carried out on cytochrome *c* that has been chemically cleaved at methionine-65 (located at the left lower rear of the molecule shown in Figure 2). An additional change that might accompany the transition to the more rigid reduced molecular state is a change in the state of hydration of the closely packed, positively charged groups at the front molecular surface (82, 83). This view tends to ascribe much of the observed negative entropy change (76) associated with reduction to water-ordering effects (84), and might explain both the oxidoreduction-coupled ion-binding properties of cytochrome *c* and the differences in surface-associated solvent shown by the reduced *minus* oxidized electron-density difference maps of these molecules (10, 12).

CONCLUDING REMARKS

Overall, the available data present a reasonably consistent picture suggesting that the soluble high-potential cytochromes *c* form a relatively weak complementary charge-mediated interaction with the biological membrane containing their physiological oxidoreductants (85). They are consequently free to undergo two-dimensional diffusion on the membrane surface, which brings them into alternate contact with their membrane-bound oxidoreductases (86). The surface positive-charge localization on the cytochrome *c* molecule serves to orient the molecule such that its heme prosthetic group makes direct and alternate interactions with the prosthetic groups of the oxidoreductases (Figure 14). Although it has been suggested that mitochondrial cytochrome *c* might make simultaneous interactions with its oxidase and reductase at the membrane surface (3), the previously described model studies (Figure 13) suggest that this is a structural impossibility. Rather it appears that the reversible binding of the oxidized and reduced cytochromes *c*, which is accompanied by changes in affinity for biologically significant anions (e.g. ATP, PO_4^{2-}), provides a means by which the overall transfer of electrons to the terminal oxidant may be physiologically controlled (3).

Despite the knowledge of the tertiary structure of several cytochromes *c*, the structural features responsible for conferring reactive specificity on

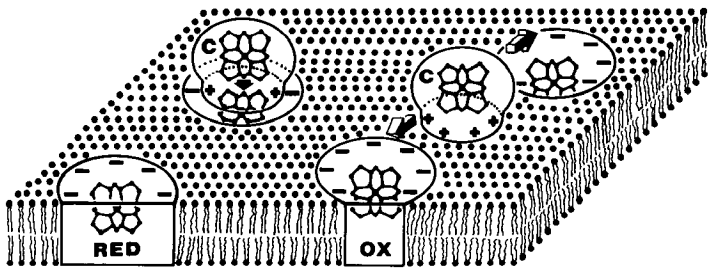

Figure 14 A schematic drawing showing the probable nature of the interactions made between cytochromes *c* and their membrane-bound oxidases (OX) and reductases (RED). Cytochrome *c* is peripherally bound on the membrane surface by complementary charge interactions formed between a ring of positively charged residues about the perimeter of its heme crevice and the negatively charged membrane surface and/or membrane-bound oxidoreductase. The ionic interaction formed between the cytochrome *c* molecule and the membrane is relatively weak, giving the cytochrome *c* two-dimensional mobility (arrows) such that it may reversibly and alternately interact with its physiological oxidoreductases. The complementary ionic interactions serve to orient the cytochrome *c* molecule so that it is oxidized (shown) or reduced by a mechanism involving direct interaction of the cytochrome *c* heme and prosthetic groups of its oxidoreductases.

these molecules are not currently understood. The possibilities include (*a*) subtle differences in the number and location of surface charges, which alter the binding characteristics of the cytochrome to the oxidoreductase or affect its relative structural stability in the oxidized and reduced states; (*b*) surface structural differences, which might affect attainment of the proper relative orientations of prosthetic groups [e.g. the mitochondrial cytochromes *c* possess an invariant Gln 16 at the surface adjacent to the heme crevice, whereas *P. denitrificans* c_{550} and the bacterial cytochromes c_2 lack both this residue and high reactivity with the mitochondrial oxidase (2)]; and (*c*) differences in specific mechanisms of facilitation of the oxidoreduction reaction. Hopefully, structural studies in progress on the smaller prokaryotic high-potential cytochromes *c*, as well as on other heme proteins serving electron-transfer functions (87, 88), will provide the structural data base required to discriminate between these possibilities.

ACKNOWLEDGMENTS

Thanks are due to Drs. R. P. Ambler, R. G. Bartsch, M. A. Cusanovich, R. E. Dickerson, M. D. Kamen, and E. Margoliash, who provided preprints and information prior to publication. Work in this laboratory is supported by the National Science Foundation (BMS75–06558), the National Institutes of Health (GM21534), and the Research Corporation.

Literature Cited

1. Salemme, F. R., Kraut, J., Kamen, M. D. 1973. *J. Biol. Chem.* 248:7701–16
2. Dickerson, R. E., Timkovich, R. 1976. *The Enzymes* 11:397–547
3. Ferguson-Miller, S., Brautigan, D. L., Margoliash, E. 1977. In *The Porphyrins*, ed. D. Dolphin. New York: Academic. In press
4. Cusanovich, M. A. 1977. *Bioorganic Chem.* In press
5. Bartsch, R. G. 1977. In *The Photosynthetic Bacteria*, ed. R. K. Clayton, W. R. Sistrom. New York: Plenum. In press
6. Ambler, R. P., Meyer, T. E., Kamen, M. D. 1976. *Proc. Natl. Acad. Sci. USA* 73:472–75
7. Dickerson, R. E., Timkovich, R., Almassy, R. J. 1976. *J. Mol. Biol.* 100:473–91
8. Swanson, R., Trus, B. L., Mandel, N., Mandel, G., Kallai, O. B., Dickerson, R. E. 1977. *J. Biol. Chem.* 252:759–75
9. Takano, T., Trus, B. L., Mandel, N., Mandel, G., Kallai, O. B., Swanson, R., Dickerson, R. E. 1977. *J. Biol. Chem.* 252:776–85
10. Salemme, F. R., Freer, S. T., Nguyen Huu Xuong, Alden, R. A., Kraut, J. 1973. *J. Biol. Chem.* 248:3910–21
11. Timkovich, R., Dickerson, R. E., Margoliash, E. 1976. *J. Biol. Chem.* 251: 2197–2206
12. Timkovich, R., Dickerson, R. E. 1976. *J. Biol. Chem.* 251:4033–46
13. Aviram, I., Schejter, A. 1971. *Biochim. Biophys. Acta* 229:113–18
14. Wüthrich, K., Aviram, I., Schejter, A. 1971. *Biochim. Biophys. Acta* 253:98–103
15. Kassner, R. J. 1973. *J. Am. Chem. Soc.* 95:2674–77
16. Kassner, R. J. 1972. *Proc. Natl. Acad. Sci. USA* 69:2263–67
17. Pettigrew, G. W., Meyer, T. E., Bartsch, R. G., Kamen, M. D. 1975. *Biochim. Biophys. Acta* 430:197–208
18. Redfield, A. G., Gupta, R. K. 1971. *Cold Spring Harbor Symp. Quant. Biol.* 36:405–11
19. Hodges, H. L., Holwerda, R. A., Gray, H. B. 1974. *J. Am. Chem. Soc.* 96: 3132–37

20. Marcus, R. A. 1956. *J. Chem. Phys.* 24:966–78
21. Hopfield, J. J. 1974. *Proc. Natl. Acad. Sci. USA* 71:3640–44
22. Dickerson, R. E., Takano, T., Eisenberg, D., Kallai, O. B., Samson, L., Cooper, A., Margoliash, E. 1971. *J. Biol. Chem.* 246:1511–35
23. Takano, T., Kallai, O. B., Swanson, R., Dickerson, R. E. 1973. *J. Biol. Chem.* 248:5234–55
24. Takano, T., Swanson, R., Kallai, O. B., Dickerson, R. E. 1971. *Cold Spring Harbor Symp. Quant. Biol.* 36:397–404
25. Dickerson, R. E., Takano, T., Kallai, O. B., Samson, L. 1972. In *Structure and Function of Oxidation Reduction Enzymes,* ed. Å. Åkeson, A. Ehrenberg, pp. 69–83. New York: Pergamon. 777 pp.
26. Dewar, M. J. S., Hashmall, J. A., Venier, C. G. 1968. *J. Am. Chem. Soc.* 90:1953–57
27. Dewar, M. J. S., Hashmall, J. A., Trinajstic, N. 1970. *J. Am. Chem. Soc.* 92:5555–59
28. Elsden, S. R., Kamen, M. D., Vernon, L. P. 1953. *J. Am. Chem. Soc.* 75: 6347–48
29. Davis, K. A., Hatefi, Y., Salemme, F. R., Kamen, M. D. 1972. *Biochem. Biophys. Res. Commun.* 49:1329–35
30. Pettigrew, G. W., Schejter, A. 1974. *FEBS Lett.* 43:131–34
31. Rodkey, F. L., Ball, E. G. 1950. *J. Biol. Chem.* 182:17–28
32. Morgan, W. T., Riehm, J. P. 1973. *Arch. Biochem. Biophys.* 154:415–21
33. Smith, G. M., Kamen, M. D. 1974. *Proc. Natl. Acad. Sci USA,* 71:4303–6
34. Aviram, I., Schejter, A. 1969. *J. Biol. Chem.* 244:3773–78
35. Margalit, R., Schejter, A. 1970. *FEBS Lett.* 6:278–80
36. Pettigrew, G. W., Aviram, I., Schejter, A. 1975. *Biochem. J.* 149:155–67
37. Morton, R. A., Overnell, J., Harbury, H. A. 1970. *J. Biol. Chem.* 245:4653–57
38. Yamanaka, T., Kamen, M. D. 1965. *Biochim. Biophys. Acta* 96:328–30
39. Yamanaka, T., Okunuki, K. 1968. In *Structure and Function of Cytochromes,* ed. K. Okunuki, M. D. Kamen, I. Sekuzu, pp. 390–403. Baltimore: Univ. Park Press. 743 pp.
40. Fanger, M. W., Harbury, H. A. 1965. *Biochemistry* 4:2541–45
41. Hettinger, T. P., Harbury, H. A. 1965. *Biochemistry* 4:2585–89
42. Hettinger, T. P., Harbury, H. A. 1964. *Proc. Natl. Acad. Sci. USA* 52:1469–76
43. White, G. A., Elliott, W. B. 1972. *Biochem. Biophys. Res. Commun.* 47: 1186–95
44. Wada, K., Okunuki, K. 1969. *J. Biochem. (Tokyo)* 66:249–58
45. Davies, H. C., Smith, L. C., Wasserman, A. R. 1964. *Biochim. Biophys. Acta* 85:238–46
46. Smith, L., Conrad, H. 1956. *Arch. Biochem. Biophys.* 63:403–13
47. Smith, L., Minnaert, K. 1965. *Biochim. Biophys. Acta* 105:1–14
48. Bartsch, R. G., Kakuno, T., Horio, T., Kamen, M. D. 1971. *J. Biol. Chem.* 246:4489–96
49. Salemme, F. R. 1976. *J. Mol. Biol.* 102:563–68
50. Mathews, F. S., Argos, P., Levine, M. 1972. *Cold Spring Harbor Symp. Quant. Biol.* 36:387–95
51. Mathews, F. S., Levine, M., Argos, P. 1972. *J. Mol. Biol.* 64:449–64
52. Passon, P. G., Hultquist, D. E. 1972. *Biochim. Biophys. Acta* 275:62–73
53. Strittmatter, P. 1964. In *Rapid Mixing and Sampling Techniques in Biochemistry,* ed. B. Chance, R. H. Eisenhardt, Q. H. Gibson, K. K. Lundberg-Holm, pp. 71–84. New York: Academic. 400 pp.
54. Shrake, A., Rupley, J. A. 1973. *J. Mol. Biol.* 79:351–71
55. Carter, C. W. Jr., Kraut, J., Freer, S. T., Nguyen Huu Xuong, Alden, R. A., Bartsch, R. G. 1974. *J. Biol. Chem.* 249:4212–55
56. Mizrahi, I. A., Wood, F. E., Cusanovich, M. A. 1976. *Biochemistry* 15: 343–48
57. Nozaki, M., Mizushima, H., Horio, T., Okunuki, K. 1958. *J. Biochem. (Tokyo)* 45:815–45
58. Greenwood, C., Wilson, M. T. 1971. *Eur. J. Biochem.* 22:5–10
59. Greenwood, C., Palmer, G. 1965. *J. Biol. Chem.* 240:3660–63
60. Kaminsky, L. S., Miller, V. J., Davison, A. J. 1933. *Biochemistry* 12:2215–21
61. Lambeth, D. O., Campbell, K. L., Zand, R., Palmer, G. 1973. *J. Biol. Chem.* 248:8130–36
62. Wilson, M. T., Greenwood, C. 1971. *Eur. J. Biochem.* 22:11–18
63. Stellwagen, E. 1964. *Biochemistry* 3: 919–23
64. Kaminsky, L. S., Burger, P. E., Davison, A. J., Helfet, D. 1972. *Biochemistry* 11:3702–6
65. Schejter, A., Aviram, I. 1969. *Biochemistry* 8:149–53
66. Schejter, A., George, P. 1964. *Biochemistry* 3:1045–49

67. Ulmer, D. D., Kägi, J. H. R. 1968. *Biochemistry* 7:2710–17
68. Kägi, J. H. R., Ulmer, D. D. 1968. *Biochemistry* 7:2718–24
69. Margoliash, E., Barlow, G. H., Byers, V. 1970. *Nature* 228:723–26
70. Margalit, R., Schejter, A. 1973. *Eur. J. Biochem.* 32:500–5
71. Stellwagen, E., Shulman, R. G. 1973. *J. Mol. Biol.* 80:559–73
72. Stellwagen, E., Cass, R. D. 1975. *J. Biol. Chem.* 250:2095–98
73. Miller, W. G. Jr., Cusanovich, M. A. 1975. *Biophys. Struct. Mech.* 1:97–111
74. Margalit, R., Schejter, A. 1973. *Eur. J. Biochem.* 32:492–99
75. Margalit, R., Schejter, A. 1974. *Eur. J. Biochem.* 46:387–91
76. Watt, G. D., Sturtevant, J. M. 1969. *Biochemistry* 8:4567–71
77. Harbury, H. A., Cronin, J. R., Fanger, M. W., Hettinger, T. P., Murphy, A. J., Myer, Y. P., Vinogradov, S. N. 1965. *Proc. Natl. Acad. Sci. USA* 54:1658–64
78. Schejter, A., Aviram, I. 1970. *J. Biol. Chem.* 245:1552–57
79. Wüthrich, K., Aviram, I., Schejter, A. 1971. *Biochim. Biophys. Acta* 253:98–103
80. Corradin, G., Harbury, H. A. 1970. *Biochim. Biophys. Acta* 221:489–96
81. Corradin, G., Harbury, H. A. 1971. *Proc. Natl. Acad. Sci. USA* 68:3036–39
82. Krestov, G. A. 1962. *Zh. Strukt. Khim.* 3:137–42 (in Russian)
83. Krestov, G. A. 1962. *Zh. Strukt. Khim.* 3:402–10 (in Russian)
84. Lumry, R., Rajender, S. 1970. *Biopolymers* 9:1125–227
85. Vanderkooi, J., Erecińska, M., Chance, B. 1973. *Arch. Biochem. Biophys.* 154: 219–29
86. Wagner, M., Erecińska, M. 1971. *Arch. Biochem. Biophys.* 147:666–74
87. Salemme, F. R. 1974. *Arch. Biochem. Biophys.* 163:423–25
88. Czerwinski, E. W., Mathews, F. S. 1974. *J. Mol. Biol.* 86:49–57

CONTENTS